

# **P&ID-based automated fault identification for energy performance diagnosis in HVAC systems: 4S3F method, development of DBN models and application to an ATEs system**

Arie Taal <sup>a</sup>, Laure Itard <sup>b</sup>

<sup>a</sup> Department of Mechanical Engineering, The Hague University of Applied Sciences, Delft, The Netherlands

<sup>b</sup> Research Institute OTB, Delft University of Technology, Delft, The Netherlands

## **Abstract**

Current methods for energy diagnosis in heating, ventilation and air conditioning (HVAC) systems are not consistent with process and instrumentation diagrams (P&IDs) as used by engineers to design and operate these systems, leading to very limited application of energy performance diagnosis in practice. In a previous paper, a generic reference architecture – hereafter referred to as the 4S3F (four symptoms and three faults) framework – was developed. Because it is closely related to the way HVAC experts diagnose problems in HVAC installations, 4S3F largely overcomes the problem of limited application. The present article addresses the fault diagnosis process using automated fault identification (AFI) based on symptoms detected with a diagnostic Bayesian network (DBN). It demonstrates that possible faults can be extracted from P&IDs at different levels and that P&IDs form the basis for setting up effective DBNs. The process was applied to real sensor data for a whole year. In a case study for a thermal energy plant, control faults were successfully isolated using balance, energy performance and operational state symptoms. Correction of the isolated faults led to annual primary energy savings of 25%. An analysis showed that the values of set probabilities in the DBN model are not outcome-sensitive.

Keywords:

Energy Performance, FDD, AFI, 4S3F method, DBN, HVAC systems

Abbreviations

AFI	automated fault isolation
AHU	air handling unit
ATES	aquifer thermal energy storage
BEMS	building energy management system
BMS	building management system
cw	cold water
DBN	diagnostic Bayesian network
EP	energy performance
F	fault
FDD	fault detection and diagnosis
HVAC	heating, ventilation and air conditioning
hp	heat pump
hw	hot water
load	load of cold water into the cold well of the ATES system
OS	operational state
PCA	principle component analysis
P&ID	pipng & instrumentation diagram
pr	primary
reg	regeneration
S	symptom
syst	system
TC	temperature controller
THUAS	The Hague University of Applied Sciences
TSA	heat exchanger
TT	temperature transmitter
unload	unload of cold water from the cold well of the ATES
4S3F	four symptoms and three faults

Symbols

COP	coefficient of performance
E	energy
EER	energy efficiency ratio
Etha	efficiency
P	power
	probability
PER	primary energy ratio
SCOP	seasonal coefficient of performance
T	temperature
$\eta$	efficiency

## 1. Introduction

As noted in [1], for example, fault detection is the detection of the presence of faults in the functioning of a system by means of symptoms. To use healthcare as an analogy, faults can be seen as illnesses which lead to symptoms. These faults are isolated and evaluated in the diagnosis process.

Despite the many studies of building commissioning and energy management, building energy analysis systems with fully automated fault detection and diagnosis are rarely applied in practice, resulting in unnecessarily high energy consumptions.

In [2] a first draft of the 4S3F method was presented. This method, based on data provided by the Building Management System (BMS), aims to achieve automated continuous energy diagnosis of complex heating, ventilation and air conditioning (HVAC) systems using a systematic approach based on the information contained in process & instrumentation diagrams (P&IDs) and the subsequent analysis of four categories of symptoms and three categories of faults (4S3F). This 4S3F method is present in the Building Energy Management System (BEMS), which can either be a separate application or be implemented in the BMS. The method was shown to overcome the problem of energy diagnosis systems seldom being used in practice because their design does not reflect how HVAC designers work. Furthermore, the process of using energy diagnosis to isolate faults is far from fully automated at present, there is little standardization of energy diagnosis and few generic methods are applicable which can be applied regardless of the type of HVAC system. This leads to solutions which are not only very specific to particular HVAC systems, but which are also time-consuming to implement.

In [2], a first draft of the 4S3F architecture was tested on a simple theoretical case. In the current article, the diagnosis phase in the 4S3F method is applied to a thermal energy plant with real sensor data for a whole year, in the assumption that symptoms have already been identified at this stage.

A great deal of research has been conducted on automated fault detection and diagnosis (FDD). Kim and Katipamula presented in [3] an overview of existing FDD methods for HVAC systems. Various diagnosis methods can be applied depending on the detection method. In the last decade, data-driven detection methods have been discussed, such as those based on regression formulas, artificial neural networks (ANN), principal component analysis (PCA) and support vectors, such as the support vector machine (SVM). Wang and Xiao [4] and Beghi et al. [5], for example, isolated sensor faults after PCA detection by means of the sensor contribution to the symptom. Li et al. [6] also estimated the contributions of possible faults to the symptom for the purpose of isolating faults. They used a support vector data description (SVDD) algorithm on chiller FDD to detect a symptom. In [7], Wang and Cui also applied PCA as a detection method and isolated the faults by means of rules using a fault diagnostic classifier.

Due to the data-driven nature of these machine learning techniques, their application to the identification of faults remains a complex process. Furthermore, these approaches to diagnosis depend on the specific method of data-driven detection applied. In addition, they rely on the availability of data on healthy operation and, for some methods, data on healthy operation combined with data on incorrect operation with known faults. Liang and Du [8], for example, applied an SVM classifier based on both normal and faulty conditions.

Besides data-driven methods, the application of model-based and rule-based methods is also commonly found in recent literature. Song et al. propose in [9] a model-based method in which faults are estimated by means of simulation, with a classification set up on the basis of the calculated symptoms. In rule-based detection methods, we see that the isolation of faults mainly takes place using a diagnosis rules table (see e.g. Zhao [10]). In DABO [11], an FDD application, rule tables are also used to isolate faults. Another method is a reference-based approach that compares the behaviour of similar components to isolate a faulty component. See [12] where this is applied to district heating substations. Despite the many solutions proposed, an approach to generic automated fault diagnosis that can be applied regardless of the type of HVAC system has yet to be developed, and the practical implementation of current methods calls for considerable effort. In particular, the IT-based nature of data-driven methods means that by their very nature they are far removed from the professional practice of HVAC engineers. Furthermore, HVAC systems are also becoming more complex due to the many possible combinations of components and complex controls that incorporate a large number of sensors. Generic FDD methods are not available for these new systems. Moreover, HVAC systems consist of subsystems and a simultaneous diagnosis for these subsystems has yet to be proposed. In research, FDD takes place sequentially either top-down or bottom-up, but not in both directions, which could help enable quicker, more comprehensive and more accurate diagnoses. In addition, all methods provide a true-false result for faults and this can lead to incorrect conclusions due to inaccuracies in measurements and method.

In the 4S3F FDD architecture, the fault isolation part of the diagnosis is carried out using

a diagnostic Bayesian network (DBN) method that largely solves these problems. The DBN method has been applied successfully to chillers [13], to VAV terminals [14] and to AHU [15 and 16]. However, these applications are still HVAC-specific. The automated fault isolation (AFI) in the 4S3F method overcomes this problem and has been demonstrated at the extensive thermal energy plant at The Hague University of Applied Sciences (THUAS) building in Delft, the Netherlands, using the data present in the building's BMS. The HVAC system that formed the focus of the study contains a gas boiler and a heat pump combined with an aquifer thermal energy storage (ATES) system for storage and supply of both heat and cold. All buffers and hydronic systems were also included. The analysis covers a whole year, based on data collected at 16-minute intervals, and demonstrates the practical usability of the 4S3F architecture for an existing HVAC system.

The basic 4S3F diagnosis architecture for energy performance is briefly presented in Section 2. In Section 3 the generic approach of AFI with the 4S3F approach is presented. Section 4 describes the HVAC system under consideration. In Section 5 the symptoms detected in the case study are presented, as they form the starting point for the fault diagnosis method. Section 6 describes the application of the AFI method applying DBN models. In this section the case study results are presented and evaluated and in section 7 the fault diagnosis without subsystems and fewer symptoms is discussed. Section 8 energy optimization and savings are discussed. Additionally, in Section 9, a sensitivity analysis is conducted on prior probabilities in the case study. Finally, in Section 10, conclusions are drawn and recommendations made concerning the fault diagnosis

element of the 4S3F diagnosis framework.

## 2. 4S3F architecture for energy performance detection and diagnosis

This section presents the salient points of the 4S3F architecture. For a detailed explanation of this architecture, see [2].

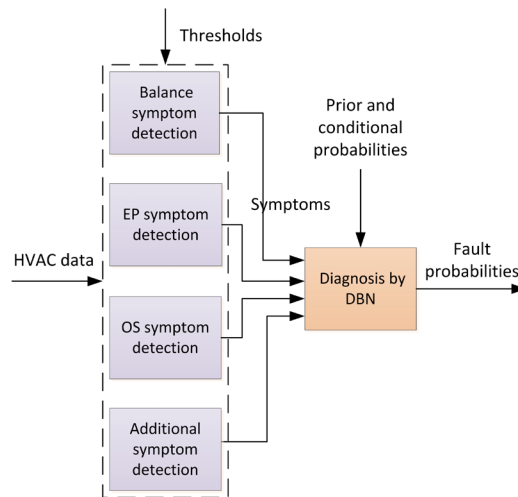


Fig. 2.1 4S3F architecture for automated energy performance detection and diagnosis

The identification of symptoms starts with the detection of observable malfunctioning symptoms, based on the HVAC P&IDs (process and instrumentation diagrams) and the measurement points and set points present in the BMS, the main purposes of which are the control and monitoring of the HVAC system.

These symptoms are categorised in four main types (4S), see Fig 2.1: balance symptoms (energy, mass and pressure-based), energy performance (EP) symptoms, operational state (OS) symptoms and additional symptoms (based on additional information such as maintenance information). The results of the symptom detection phase are supplied to a

diagnostic Bayesian network (DBN) model. In this model, symptoms are linked to possible faults. We distinguish three types of faults: faults in the models used to enrich BMS data (e.g. to estimate missing energy data or to set up balance models), component faults and faults affecting control components. In this paper, we demonstrate a DBN for energy performance purposes, in which we have taken into account that model faults are not present and that this has been checked. We define components as being not only trade components but also HVAC systems at different aggregation levels. Fig. 2.2 shows the relationship between the four types of symptoms and the three types of faults as implemented in the 4S3F DBN models. The direction of the arrows in the DBN runs from the fault nodes to the symptom nodes. In other words, this figure shows which symptoms may be caused by a specific fault. The components and controls can be extracted from the HVAC P&ID diagram. The present paper focuses solely on the fault identification part (3F) of the 4S3F framework.

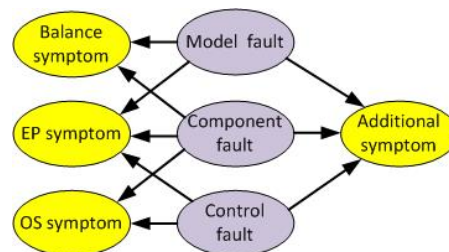


Fig. 2.2 4S3F DBN structure

In the DBN diagnosis, the Present and Absent probabilities of the faults are estimated on the basis of the presence and absence of symptoms as established by the symptom detection.

The main advantages of applying DBN for fault isolation purposes, presented in [2], is that the structures of the DBN models can be extracted from P&IDs and that isolation of

multiple faults takes place simultaneously. This also supports a system approach, because a DBN model can be built from DBN submodels and can be set up using aggregated DBN models from a DBN model library. A DBN model is easy to expand. Due to its probability-based character, the DBN approach addresses uncertainties in measurements and in the FDD model and is to some extent insensitive to parameter values of the DBN nodes. It can handle conflicting symptoms and delivers results even when only a few symptom nodes are available because the outcomes are probabilities instead of Boolean. Furthermore, symptoms from all kinds of detection methods can be integrated.

### **3. The fault identification approach based on the 4S3F method**

This section discusses the generic approach to identify faults from symptoms applying DBN models. As explained in Section 2, many different faults can lead to a single symptom. The reverse is also true: a fault can result in multiple symptoms. It is therefore necessary to conduct an analysis of the combination of all observed symptoms to determine the exact cause(s) of malfunctioning (the fault(s)). The 4S3F fault diagnosis method, as shown in Fig. 2.1, is based on Bayesian theory. Using the detected symptoms, the probability of occurrence of specific faults can be estimated.

Just as all possible symptoms can be identified once from the HVAC schematic, so all possible faults must also be identified once for each HVAC system, based on the HVAC P&ID (see for such a diagram Fig. 4.3). This is a relatively simple once-only inventory, as was noted in [2], and will be demonstrated in Section 3.2. This inventory results in all possible faults being connected to all possible symptoms through a DBN. The structure of the DBN closely follows the structure of the HVAC P&ID and its construction (also a once-only event) is therefore reasonably straightforward. A distinction can be made between component faults, control faults and model faults, see Fig. 2.2. In the present paper, model faults are left out of the description in order to avoid excessively long descriptions and because a DBN with a model fault was already described in [2].

System levels on which DBN models are set up are discussed first, followed by how to establish the relationships between faults and symptoms from a P&ID. This chapter ends with the implementation of the DBN models.

#### **3.1 System levels**

As well for components as for controls levels are distinguished.

### Components

According to [2], we should consider components on different levels, as a simultaneous diagnosis helps to isolate faults more accurately due to redundancy:

Level A: the total system

Level B: aggregated systems

Level C: (trade) components

Level D: subcomponents inside (trade) components

This also helps to define reusable diagnostic models that may be available in a library.

For the sake of demonstration, complex DBN schematics are not shown in this paper, as

we have made a conscious effort to limit the number of DBN nodes. This means that

Level A (the complete system) and Level D (parts of components) are not shown, and

only the faults at Levels B (aggregated systems) and C (components) are included. For

instance, a malfunction in the heat pump is a possible fault but we will not specify the

exact location within the heat pump at Level D, e.g. the compressor, evaporator,

condenser or embedded control. In other words, the heat pump will be treated as a black

box system, which is logical given that it is a commercially available component. In the

authors' view, fault diagnosis at Level D could be implemented by component suppliers.

Fault results from such as diagnosis could then be used as additional symptoms in the

4S3F method. For energy diagnosis purposes, we propose that the aggregated systems are

based on generator, hydronic and emitter systems according to EN 15316-1:2017 [17].

### Controls

As with components, for the purposes of this paper faults in the control system of each system are aggregated to one fault per system: for instance, the control of the heat regeneration system may be faulty, but we do not specify whether the fault is in the temperature set point or in the timer setting. It may of course be possible and even desirable to consider both in practice, but that is not necessary to demonstrate the method within the context of this paper.

A control contains controllers which derive signals from sensors and send signals to components acting as actuators. These signals propagate information, as opposed to components which exchange energy. Control faults can be errors in controllers (e.g. control rules, set points), in connections with sensors and in actuators (e.g. broken wires and interruptions) and caused by incorrect design of the control circuit, including actuators. Generic controls at level B applied in thermal plants with an ATEs system are the control of the ATEs system, of the cold water, the hot water, and in addition, controls at Level C: the controls of the supplied condenser and evaporator water temperature of the heat pump.

The control parts of the P&ID can be based on guidelines (e.g. documents on hydronic systems, such as the ISSO standard for hydraulic systems [18 and 19]), which describe HVAC modules in the Netherlands.

### **3.2 Relationships between faults and symptoms**

In this section, generic DBN (sub)models are discussed, along with their implementation. As depicted in Section 3.1, components at Levels A to D can be defined. Generic fault isolation models can be developed once only for each type of component. The fact that this approach takes in balance, energy performance and operational state symptoms

regardless of components and controls is what makes it generic. Components at lower levels can be combined to form generic subsystems and finally to generic aggregated systems as models for the thermal generator, hydronic and emitter systems. The first step is to construct the overall DBN model using DBN models for systems at level B and C, followed by setting the prior and conditional probabilities of the fault and symptom nodes. Again, this is done only once for each model, which can be saved in a model library.

It can be helpful to create a table that lists related errors and symptoms. See for instance Table 3.1, where such a generic model has been set up for a heat pump system (a generator system) at level B. The grey filled cells indicate the presence of a relation. As example, the cause of a low COP of the heat pump may be a malfunctioning heat pump, a too high set point in the control of the outlet water temperature of the condenser or a too low set point in the control of the outlet water temperature of the evaporator. However, it can also be approached on the other hand: if a fault is present, what symptoms can there be?

Faults	Heat pump	Control outlet water temperature of the evaporator	Control outlet water temperature of the condenser
Symptoms			
Heat pumps' capacity			
COP heat pump in heating mode			
EER heat pump in cooling mode			
Outlet water temperature evaporator			
Outlet water temperature condenser			

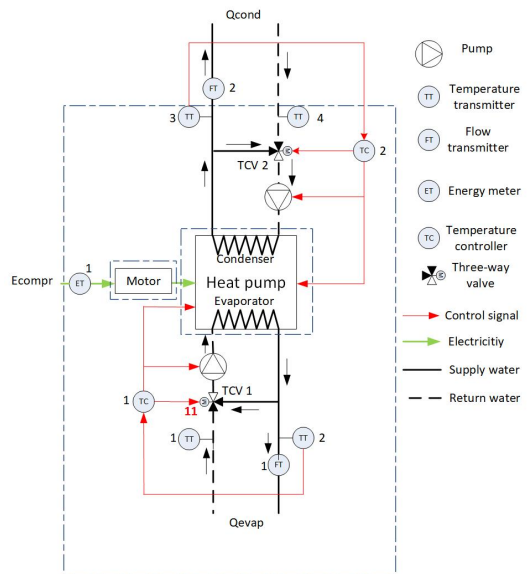


Table 3.1 Fault-symptom relation table for a heat pump system. Fig. 3.1 P&ID heat pump system.

For the purposes of simplicity and accuracy, we propose that only strong relations should be set up and weak ones should be ignored. Such tables can easily be set up with reference to the HVAC P&ID (which depicts components at level B) as shown in Fig. 3.1. In this figure, we see the controllers TC1 and TC2 which controls the evaporator outlet temperature (measured by sensor TT2) and the condenser outlet temperature (measured by TT3). The heat pumps' capacity is estimated by the temperature sensors TT3 and TT4, and the flow sensor FT2. The COP (coefficient of performance) is calculated from the supplied heat  $Q_{cond}$  and the compressor work  $E_{compr}$ , measured by ET1. And the EER (energy efficiency ratio) by the supply cold  $Q_{evap}$  and  $E_{compr}$ . Thus, we see that from the P&ID we can extract faults as well symptoms.

### **3.3 DBN models**

As stated in Section 2, the DBN model calculates the posterior fault probabilities from the presence and absence of symptoms. An example of such a calculation is given in Appendix B of [20].

#### DBN schematics

From the relationships between the faults and symptoms, a DBN model is set up. As example, Table 3.1 results in the DBN model shown in Fig. 3.2.

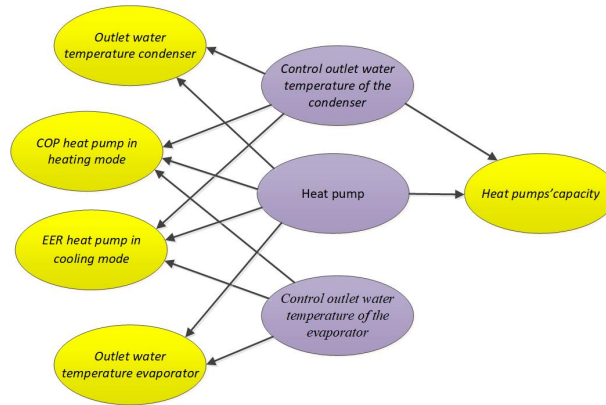


Fig. 3.2 DBN schematic diagram of a heat pump system.

Since DBN models of aggregated systems at Level B as shown in Fig. 3.2 are generic, this can be done once and then be reused.

The software tool we used to construct our models is called GeNie [21]: a validated software application offering the possibility to create aggregated DBN models based on DBN submodels. This makes it possible to develop specific DBN models with the use of generic DBNs for components or systems, which shorten the implementation effort in the fault identification layer. Balance, energy performance and operational state symptom nodes are linked to fault models, such as heat pumps, boilers, cold water systems, hydronic systems and ATEs systems. The links between fault and symptom nodes can be set up once only. Some links for faults and symptoms which concern several systems and components can be set up once only for well-known system configurations. These DBN models can be stored in a library.

#### Node states and probabilities

The parameters of DBN models are probabilities for the node states. The fault nodes are so-called parent nodes which contain prior probabilities for the state of the nodes. The

corresponding child nodes, the symptom nodes, have conditional state probabilities that depend on the state of the connected parent nodes. First, the values of the prior probabilities must be set, followed by those of the conditional probabilities (see also [2], which proposes distinguishing between two states for the fault and symptom nodes: Present or Absent). The values only need to be set once when implementing the DBN model and can be based on HVAC expertise and later on historical data from the BMS.

- Prior probabilities of parent nodes

The absolute values of the prior Present and Absent probabilities for the events are chosen arbitrarily but their relative values are based on expert knowledge. For the sake of simplicity, we set separate fixed values for component faults and for control faults. The actual prior probabilities of component faults are set at 98%, which means that two out of 100 components are not functioning properly. However, the Absent prior probabilities of control rules are set lower to 95% because in practice energy performance often decreases due to faulty set control rules, changes in building use or incorrect changes to set points of the control system.

Fig. 3.3 presents an example of the prior properties of a fault called *Control roof heating*. We distinguish between two states: Present or Absent with corresponding probabilities.

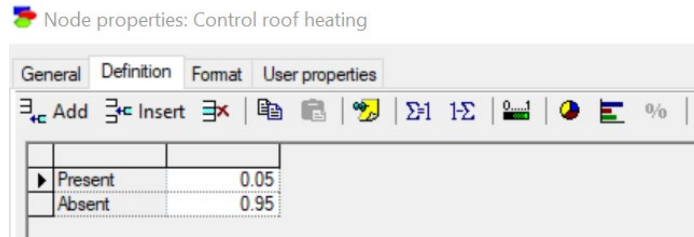


Fig. 3.3 The implemented prior node properties of a fault called *Control roof heating* in GeNie

- Conditional properties of child nodes

The probabilities of the Present and Absent states of the symptom nodes depend on the state values of the fault nodes. In this case study, it is assumed that when one of the parents is Present, the child value is Present with an arbitrary probability of 95%. This means there is an Absent probability of 5% for the child node when one or more of the parents are Present, because parent node faults can cancel each other out and lead to no symptom.

By way of example, Fig. 3.4 presents the set properties in the dialogue box of a symptom node, in this case for a symptom called *SEERcw*. We have applied so-called Noisy-MAX nodes, in which we assume that the symptom is Absent when all parent states are Absent (LEAK=1).

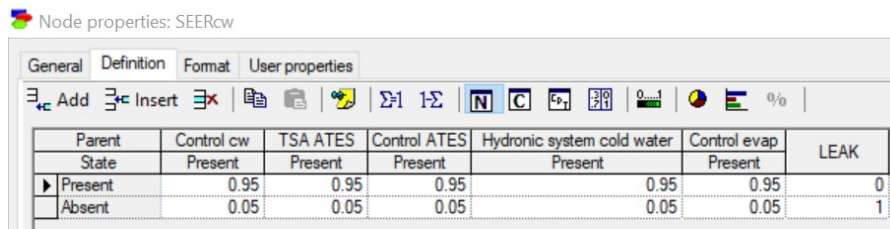


Fig. 3.4 The implemented conditional node probabilities of a symptom called *SEERcw* in GeNie.

In future, the prior and conditional probabilities can be estimated more precisely as a result of experience and data mining. However, [20], in which the 4S3F method was conducted on a demand controlled ventilation system, showed that the absolute values of the set probabilities are somewhat insensitive for the diagnosis results. In Section 9 we confirm that rough-set prior probabilities do not influence the outcomes fundamentally.

#### 4. The thermal energy plant at The Hague University of Applied Sciences in Delft

The identification part of the 4S3F method is tested on the HVAC system of the THUAS building in Delft (see Figs. 4.1 and 4.2). The ventilation of the building rooms is demand controlled by CO<sub>2</sub> concentration. In the classrooms and general living areas there is underfloor heating and cooling and in the staff rooms this has been extended with heat and cold ceiling panels.



Fig. 4.1 The atrium of the THUAS building.



Fig. 4.2 A staff room in the THUAS building.

Below we present a short description of the thermal energy plant. The P&ID of the thermal energy plant is presented in Fig. 4.3. For the sake of simplicity controllers are not depicted.

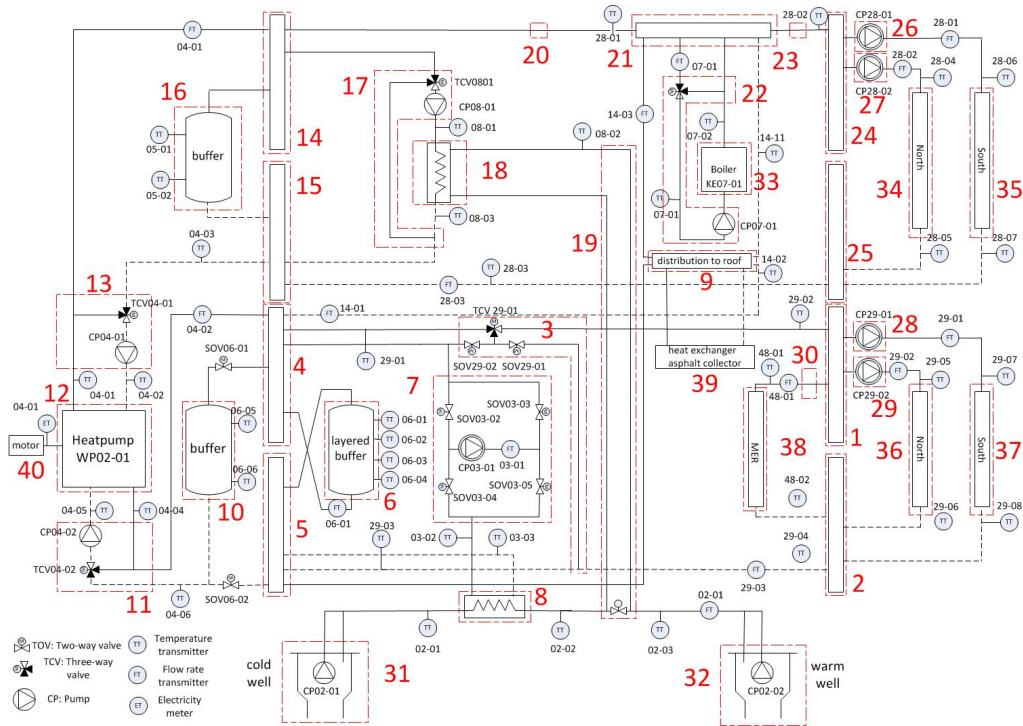


Fig. 4.3 Principal diagram (P&ID) of the thermal energy plant at THUAS

Fig. 4.4 shows the heat exchanger (8) with at the left a part the heat pumps' casing and in Fig. 4.5 the headers (14) and (15) are presented.



Fig. 4.4 The heat exchanger (8)



Fig. 4.5 The headers (14) and (15)

We have simplified this diagram based on generator, hydronic and emitter systems at level B. See Fig. 4.6, in which relevant energy variables used for symptom detection are also depicted. In this figure, controllers for hot and cold water supply temperatures ( $TC_{hw}$  and  $TC_{cw}$ ), roof heating ( $TC_{roof}$ ), regeneration ( $TC_{reg}$ ) and ATEs ( $TC_{ATES}$ ) systems. Coupled control and sensor signals are also shown. These controls are explained in Section 6.1. Annual energy flows and efficiencies measured in 2013 are also depicted.

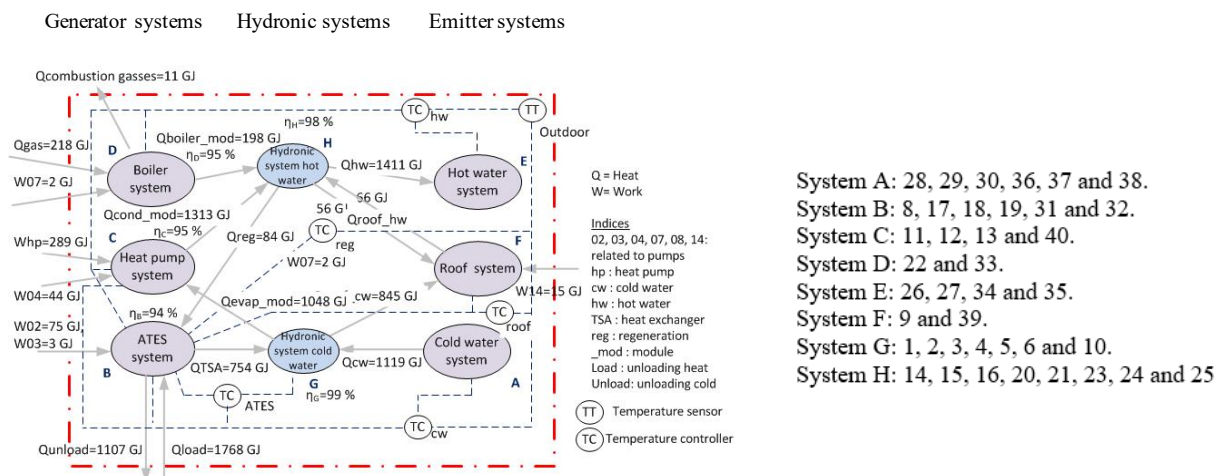


Fig. 4.6 The relevant aggregated systems at Level A (red dotted line, whole system) and at Level B (consisting of systems A to H), and system controls

In this figure, eight aggregated systems are present, based on systems 1 to 40 depicted in Fig. 4.3. The determination of systems and subsystems is a one-off task, carried out based on the P&IDs as explained in [2].

In winter, heat is generated by a heat pump. When the heat loads are high, a gas boiler delivers additional heat. The heat source of the heat pump is warm water delivered by the warm well of an ATES system, which presents the winter mode of the thermal energy generation system in a schematic. The ATES system can also deliver heat to the parking lane on the roof to keep it free of ice.

In the summer months, cold water from the cold well of the ATES system provides cooling. When cooling loads are high, the heat pump produces additional cold water on the evaporator side. This type of thermal energy plant with an ATES system is common in the Netherlands: more than 2,000 of them have been installed in recent years and their operation is known to be often sub-optimal.

During the summer, heat from the heat pump condenser and the roof collector can be used to regenerate the warm well of the ATES system because the amount of thermal energy extracted from and supplied to the wells must be balanced annually in accordance with Dutch regulations. In Fig 4.6 the direction of the arrows shows positive heat transfer. Work supplied by pumps and the heat pump compressor is noted as  $W$  in these figures. Measurement data are stored in the BMS at 16-minute intervals. The codes of the sensors and actuators (from 02 to 48) as implemented in the BMS were supplied by the designer of the HVAC system. As example, Fig. 4.7 shows the flow sensor with code FT28-03 which is located in the hot water circuit depicted in Fig. 4.3.



Fig. 4.7 Flow sensor FT28-03

For the case study, the whole of the year 2013 is included due to the availability of an almost complete dataset.

## 5. Detected symptoms in the case study

In this section, the symptoms detected by the 4S3F method in the year of 2013 are listed and form the starting point for the AFI. Table 5.1 summarises the annual results of the symptom detection process conducted in the case study. To estimate the presence or absence of a particular symptom, BMS sensor data are used. In a separate process, sensor data outliers are left out and missing data are filled in. Furthermore, biased data are corrected (also using the 4S3F method). This means that the data available is faultless. Symptoms concerning efficiencies ( $\eta$ ) constitute thermal energy losses in systems which are required to be lower than 2-4%, depending on the system. In addition, Table 5.1 shows the efficiency of the TSA heat exchanger of the ATES system  $\eta_{TSA}$  (87% according to design) and the efficiency of the thermal energy regeneration of the ATES system  $\eta_{reg}$ , which Dutch regulations stipulate must be 100% (i.e. each year, the same amount of thermal energy must be supplied to the aquifer as is used). These are defined as balance symptoms because they are calculated on the basis of energy balances. In addition to balance symptoms, we also identify energy performance and operational state symptoms. The first are related to performance indicators such as the seasonal performance coefficient (SCOP) for the generation of thermal energy (a threshold of -5% is taken into account) and capacities (P) of components and systems realized as compared to those specified in the design (threshold of -10%). The second are symptoms regarding actual state values such as temperatures. Here we distinguish between controlled-based state values, which are set in a control system, and rule-based state values, which are those expected on the basis of the design. In the case study, a symptom is found when a controlled or design temperature is lower or higher than needed (+/- 1 to 3 K) for more

than 10% of the days on which the associated system is operational. As Table 5.1 shows, 9 of the 31 possible symptoms of malfunctioning were shown to be present.

Table 5.1 Overview of the detection results from BMS data for the 31 possible symptoms found in the year 2013 (P= symptom present, A= symptom absent)

Balance symptoms		Energy performance (EP) symptoms				Operational state (OS) symptoms			
Efficiencies	A/ P	Performance indicators	A/ P	Capacity indicators	A/ P	Controlled-based	A/P	Design based	A /P
$\eta_{systB}$	A	<i>SCOP<sub>hw</sub></i>	A	<i>Phw</i>	A	<i>Thw<sub>supply</sub></i>	P	<i>Thw<sub>return</sub></i>	A
$\eta_{systC}$	A	<i>SEER<sub>cw</sub></i>	A	<i>Pcw</i>	P	<i>Tcw<sub>supply</sub></i>	P	<i>Tcw<sub>return</sub></i>	A
$\eta_{systD}$	A	<i>SCOP<sub>roof</sub></i>	P	<i>Php</i>	A	<i>Tcond<sub>out</sub></i>	A	<i>Tevap<sub>in</sub></i>	A
$\eta_{systG}$	A	<i>SCOP<sub>reg</sub></i>	A	<i>Proof</i>	A	<i>Tevap<sub>out</sub></i>	A	<i>Tcold<sub>well<sub>out</sub></sub></i>	A
$\eta_{systH}$	A	<i>SCOP<sub>hp</sub></i>	A	<i>Preg</i>	A	<i>Tcold<sub>well<sub>in</sub></sub></i>	P	<i>Twarm<sub>well<sub>out</sub></sub></i>	P
$\eta_{TSA}$	A	<i>SEER<sub>hp</sub></i>	A	<i>PTSA</i>	P	<i>Twarm<sub>well<sub>in</sub></sub></i>	P		
$\eta_{reg}$	P			<i>Pboiler</i>	A				

B=ATES, C=heat pump, D=boiler, G=hydronic cold water, H=hydronic hot water, hp= heat pump, hw=hot water, cw= cold water)

### Energy balance symptoms

Regeneration efficiency symptom  $\eta_{reg}$  was Present. This indicator represents the degree of thermal energy balance in the ATES system.

### Energy performance symptoms

Symptom *SCOP<sub>roof</sub>* was Present, indicating that the roof heating system used more energy than expected. Furthermore, the thermal capacities of the cold water system A

( $P_{cw}$ ) and of the heat exchanger of the ATES system ( $PTSA$ ) were lower than expected from the design values.

### **Operational state symptoms**

In addition to the balance and EP symptoms, OS symptoms were detected: the hot water supply temperature to system H was too low and the cold water supply temperature to system A too high. Unexpected temperatures were also found at the warm and cold wells of the ATES system.

## 6. Automated fault isolation in the case study

In this section, the AFI is conducted in the THUAS case study. The considered faults are discussed in Section 6.1. Section 6.2 presents the relationships between faults and symptom. Next, the implementation of the DBN models are presented in Section 6.3. And finally, in Section 6.4, the results of the fault isolation process.

### 6.1 Selected component and control faults

In aggregated hydronic systems A, E, G and H, we assume that only one fault can be present which covers faults in pipes, valves, heat exchangers, headers and pumps. In the other aggregated systems, multiple component faults are present. In the roof system F, faults in the roof collector (*TSA roof*) and hydronic system F can be present; in the heat pump system C, the heat pump (12) and the hydronic system can be present; in the boiler system D, we assume that the hydronic system D and the boiler can be faulty, and in the ATES system B, faults in the heat exchanger TSA (8) and hydronic system B are present. In total, therefore, there are 11 possible component faults to consider.

### Control faults

From the control description of the thermal energy plant, which was present in the design document and the P&ID, the following five control faults at Level B, as depicted in Fig. 4.6, can be distinguished:

- *Control ATES*
- *Control heat regeneration*
- *Control roof heating*
- *Control cw*

- *Control hw*

In addition, we take into account two controls at Level C in the heat pump system (system C):

- *Control cond*
- *Control evap*

We explain the implemented controls in the thermal energy plant of THUAS below in greater detail for the ATES and regeneration systems. The other five are described in Appendix A.

### ***Control ATES***

*Control ATES* depicts the faulty control of the ATES system. Fig. 6.1 presents a simple schematic of the control of the ATES system B. When unloading cold water, the controller of the ATES system controls the flow rate of pump CP02-01 in the cold well to obtain the desired supply temperature in the warm well, measured by TT02-03. In the same way, the temperature of the supply water to the cold well is controlled when unloading heat from the ATES.

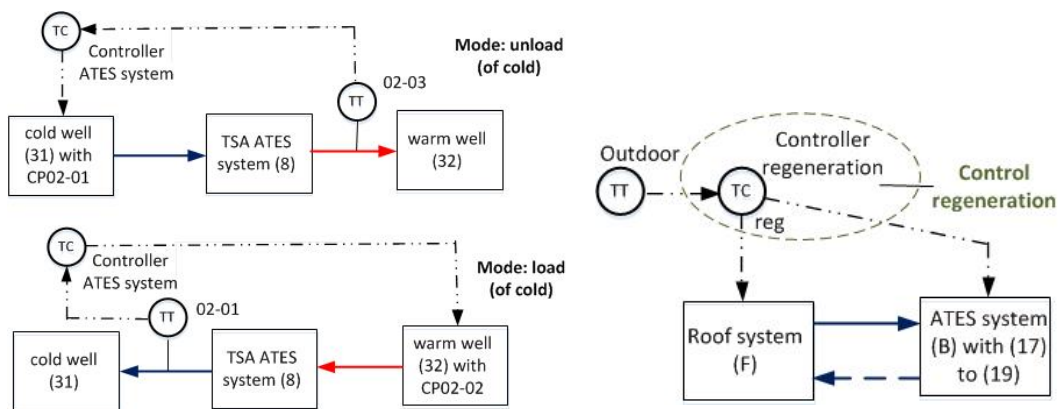


Fig. 6.1 Control of the ATES system

Fig 6.2 Control of the regeneration system

### ***Control regeneration***

*Control regeneration* depicts the control of the heat regeneration for the ATES system.

The schematic of this control is shown in Fig. 6.2. At high outdoor temperatures in summer, the roof and ATES systems are switched on. The roof system supplies heat to warm well 32 via systems 17 to 19.

### **6.2 Relationships between faults and symptoms.**

We will examine 11 possible component faults. In addition, seven control faults are present. As seen in Table 5.1, 31 outcomes for symptoms are present. A DBN model is therefore built with 18 fault nodes and 31 symptom nodes.

Table 6.1 presents the completed Table 3.1 for the case study. As noted in Section 3.2 weak relations between faults and symptoms are ignored. For instance, the relation between the heat pump capacity *Php* symptom and the *Control ATES* fault: the table supposes no relation between the two because the warm water well temperature is thought always to be high enough to deliver heat to the evaporator of the heat pump. Only if the warm water well temperatures were to drop to an unrealistically low level (e.g. 4°C) would the heat pump be incapable of delivering enough heat.

Table 6.1 Main relations between the 31 symptoms and the 18 faults to build the DBN models  
 hp= heat pump, hw=hot water, cw= cold water)

Component and control faults at Level B (aggregated systems A to H)	Control supply temperature	Hydronic system hw E	Control supply temperature cw	Hydronic system cw A	Heat pump system C				Boiler system D	Control roof system F	Roof system F	Control A TES system	ATES system B	Control regeneration	Hydronic system HWH	Hydronic system HW G
	Control outlet temperature condenser	Control outlet temperature evaporator	Heat pump 12	Hydronic system C	Boiler 33	Hydronic system D	TSA roof 39	TSA A TES 8	Hydronic system B	Control regeneration	Hydronic system HWH	Hydronic system HW G				
Symptoms																
$\eta_{systB}$																
$\eta_{systC}$																
$\eta_{systD}$																
$\eta_{systG}$																
$\eta_{systH}$																
$\eta_{reg}$																
$\eta_{TSA}$																
SCOP <sub>hw</sub>																
SEER <sub>cw</sub>																
SCOP <sub>roof</sub>																
SCOP <sub>reg</sub>																
SCOP <sub>hp</sub>																
SEER <sub>hp</sub>																
P <sub>hw</sub>																
P <sub>cw</sub>																
P <sub>hp</sub>																
Proof																
Preg																
PTSA																
Pboiler																
Thw <sub>supply</sub>																
Tcw <sub>supply</sub>																
Tcond <sub>out</sub>																
Tevap <sub>out</sub>																
Tin, cold well																
Tin, warm well																
Thw <sub>return</sub>																
Tcw <sub>return</sub>																
Tevap <sub>in</sub>																
Tout, cold well																
Tout, warm well																

### 6.3 The implementation of DBN models in GeNie

Based on Table 6.1, DBN models are built in GeNie. The overall DBN model is presented in Fig. 6.3 and is constructed based on Fig. 4.6. Both figures contain the eight

main aggregated systems A to H at Level B, shown in blue. Fault nodes are shown in purple while symptoms which can be caused by more than one system at Level B, see Table 6.1, are shown in yellow.

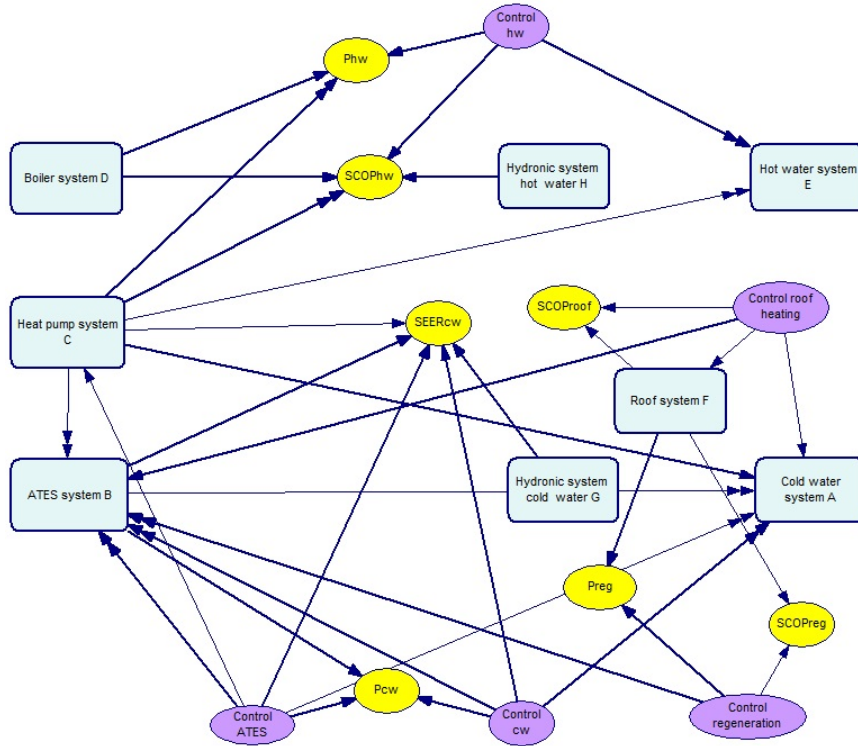


Fig. 6.3 Overall DBN model at Level B with systems A to H

Figs. 6.4 to 6.11 show the DBN models for systems A to H at Level C. As can be seen, Figs. 6.3.1 to 6.11 contain the 18 fault and 31 symptom nodes depicted in Table 6.1.

These DBN models are extracted from the P&ID of Fig. 4.3. Congruent to Fig. 2.2, the arrow directions run from the fault nodes to the symptom nodes.

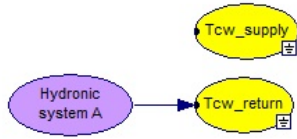


Fig. 6.4 DBN model of the cold water system A

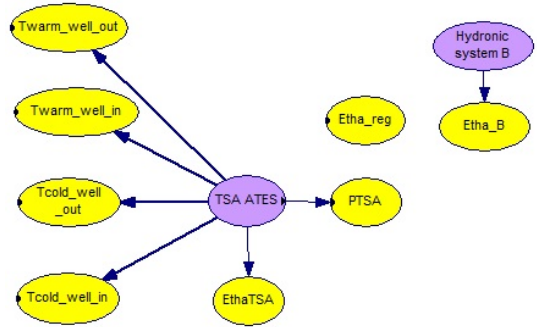


Fig. 6.5 DBN model of the ATES system B

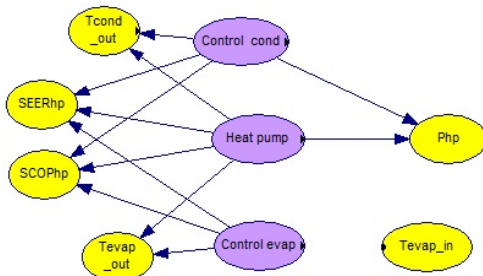


Fig. 6.6 DBN model of the heat pump system C

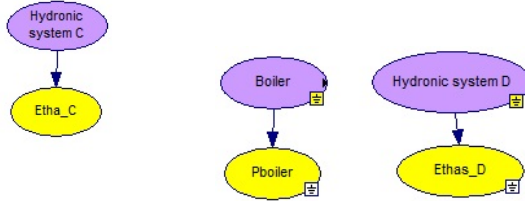


Fig.6.7 DBN model of the boiler system D

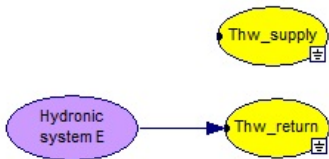


Fig. 6.8 DBN model of the hot water system E

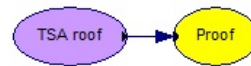


Fig. 6.9 DBN model of the roof system F

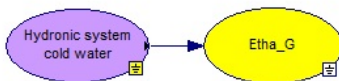


Fig. 6.10 DBN model of the cold water hydronic system G

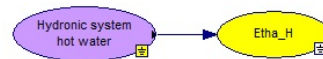


Fig. 6.11 DBN model of the hot water system H

For example, Fig. 6.5 shows that the fault node *TSA ATES* is linked to the symptom nodes  $\eta_{TSA}$ , *PTSA*, *Tcold\_well\_in*, *Twarm\_well\_in*, *Tcold\_well\_out* and *Twarm\_well\_out*, which are present in the DBN model of the ATES system. In addition, *TSA ATES* is

linked to the symptoms  $SEER_{cw}$  and  $P_{cw}$  (see Fig. 6.3), and  $T_{cw\_supply}$  and  $T_{cw\_return}$  (see Fig. 6.4). The above is consistent with Table 6.1.

### 6.4 Fault isolation results

The symptom detection results presented in Table 5.1 are imported into the DBN model. This was done manually in our case study, but it is possible to automate this process.

Note here that the symptoms were obtained using one year of 16-minute data and looking at yearly, monthly or weekly indicators. However, for the fault isolation itself, time steps are irrelevant and therefore not included in the DBN. Symptoms found over a period of less than a year (monthly, weekly, daily or even shorter timespans) can simply be fed into the DBN, resulting in shorter timespan outcomes.

We propose taking action when the Present probability outcome of a fault is higher than 30%. Isolation by the DBN resulted in four identified faults with 100% (see Fig 6.12): Present outcomes that led to 4 observed symptoms: *Control hw*, *Control ATES*, *Control regeneration* and *Control roof heating* are faulty.

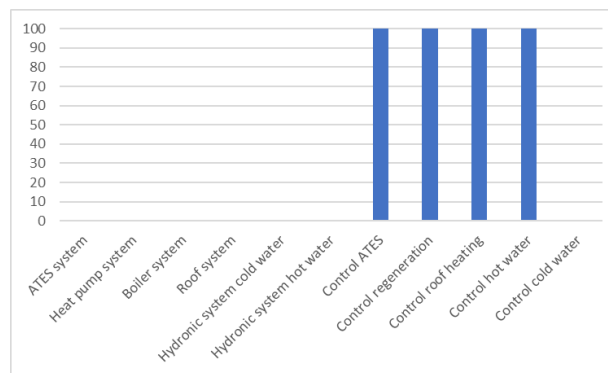


Fig. 6.12 Posterior fault probabilities.

## Discussion of the isolation results

We also contacted the maintenance company and the facility manager at THUAS to ask about other disruptions in the thermal power plant. They stated that there had been no thermal comfort complaints due to a malfunction in the thermal power plant. The four faults that were isolated would appear to be the only one's present. We will discuss them separately below.

### *Control hw*

The control fault of the hot water system was identified as Present. This diagnosis result seems to be correct because detection revealed that the supply hot water temperature was often too low. Faults were not found in the installed capacities of the heat pump and the boiler. In addition, the control of the condenser seems to be correct, because no symptom was found in the condenser outlet temperature. Apparently, an excessively low supply water temperature is caused by *Control hw*.

### *Control ATES*

The inlet water temperatures to the warm and cold well are too low and too high. As shown in Table 7.1, two main faults can cause this: *TSA ATES* or *ATES control*.

*TSA ATES* can be excluded because the efficiency of the heat exchanger efficiency  $\eta_{TSA}$  was correct. In addition, the capacity of the cold water system A was low, while no thermal comfort complaints from users had been received. It would appear that the cold water system A needs less capacity than stated in its design specifications. The resulting symptom was a lower-than-expected *PTSA* capacity. This leads to the justified conclusion

that *ATES control* has been correctly identified as faulty, leading to excessively high and excessively low load temperatures for the ATES wells.

#### *Control regeneration*

No symptom was found for the capacity of the roof collector. *TSA roof* therefore seems to be correct. However, the thermal energy balance of the ATES system was incorrect, leading to an  $\eta_{reg}$  symptom, linked to the control of the regeneration system which is identified as Present.

#### *Control roof heating*

A survey of the 16-minute energy exchange to the roof showed that the roof was also heated by the boiler. This was not in conformity with the design. Adapting the control of the roof heating would therefore appear to be a reasonable course of action.

### **7. Effects of a DBN with only aggregated systems A to H (Level B)**

The overall DBN model at aggregated Level B presented in Fig. 6.3 contains DBN models of components at Level C. In this section, we discuss DBN models for aggregated systems A to H at Level B only, with and without capacity and operational state symptoms. This is to test the importance of the combined top-down/bottom-up approach in identifying faults. Fig. 7.1 shows the DBN model with both capacity and OS symptoms. For the sake of simplicity, we have left out return water OS symptoms and efficiency symptoms. In Appendix B, DBN models at Level B without capacity or OS symptoms are also presented.

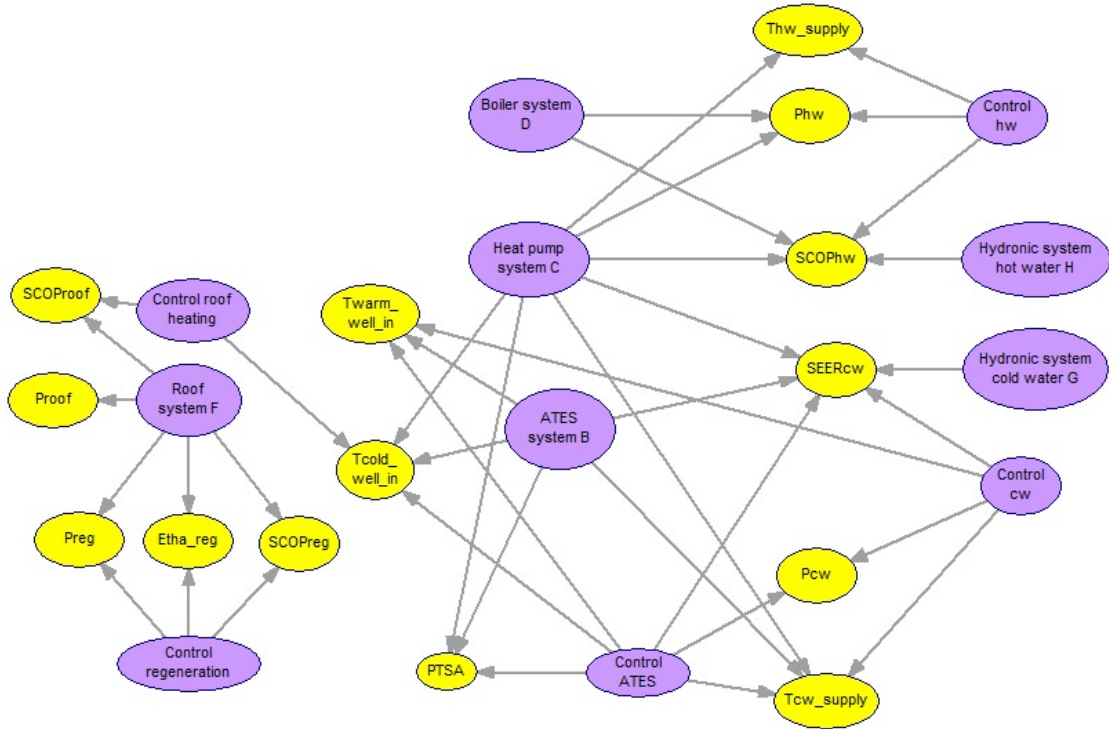


Fig 7.1 DBN model at Level B

Fig. 7.2 presents the posterior present probabilities after diagnosis. In green the results from Section 6.4 are shown. As this figure shows, diagnosis restricted to Level B (orange) shows the same outcomes as the diagnosis at Level B with DBN subsystems for components at Level C. However, it is more difficult to find a fault inside the aggregated system at Level C (e.g. the control condenser or heat pump) if the heat pump system has been isolated as a fault. Faults are not isolated correctly when capacity or OS symptoms are missing. In Fig. 7.3 these incorrect outcomes (present fault probability above 30 %) are shown with the value 1.

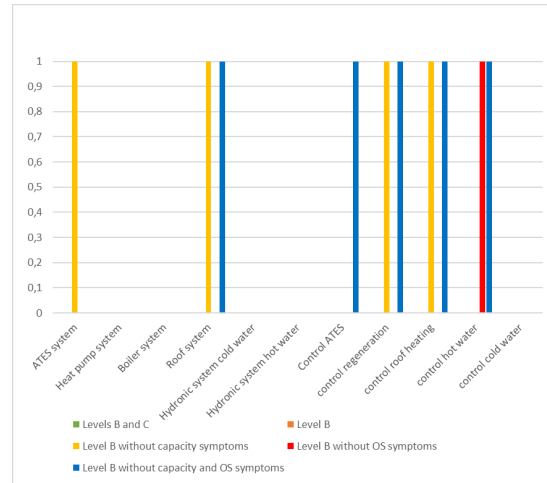
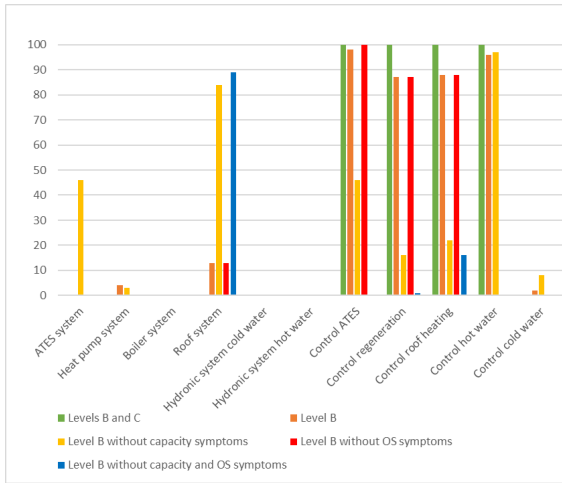


Fig. 7.2 Posterior present fault probabilities [%]

Fig. 7.3 Faulty isolation (1=faulty)

## Conclusion

Diagnosis using a DBN at Level B already delivers useful results. However, faults inside the DBN model cannot be isolated. Performance and capacity indicators, as well as operational state symptoms, are needed to isolate faults effectively. The correct and precise isolation of faults therefore requires the use of aggregated systems and their subsystems, at the same time as using multiple types of symptoms.

## **8. Fault analysis, correction and effect on energy usage**

In this section, the evaluation process after fault isolation will be discussed with reference to the case study. The primary energy savings after fault correction will also be discussed. Unfortunately, it was impossible to carry out interventions, so we can only examine the energy savings due to corrections from a theoretical perspective. However, we checked manually whether the faults found were indeed errors by analyzing the BEMS data, consulting maintenance logs, interviewing the building manager and employees of the maintenance company, so that we can say with certainty that we have not overlooked any faults. We will discuss the four faults isolated by the energy performance diagnosis separately. In the Netherlands, electricity is mainly generated by steam and gas power plants with an overall efficiency of 40%. We have taken this value into account when estimating primary energy.

Estimating energy waste and savings as a result of fault corrections is possible simply because of the availability of 16-minute data on energy levels in the BEMS.

### **8.1 Evaluation**

#### ***Fault Control hw***

As shown in Table 5.1, a symptom was detected for *Thw\_supply*, the hot water supply temperature. An excessively low supply temperature could lead to thermal comfort complaints among users of the building, but the facility management at THUAS received no complaints to this effect. Excessively high supply temperatures were supposed to lead to lower energy performance, but again no such indications emerged. We nevertheless

propose that the set values of the hot water supply controller should be checked to avoid user complaints in the future.

### ***Fault Control roof heating***

Calculations showed that part of the heat supplied to the roof was in fact supplied by the boiler (62 GJ) instead of the warm well of the ATES system. This was easy to correct by adjusting the roof control rules, and this was carried out in 2014 by the maintenance company.

### ***Fault Control regeneration***

The data suggests that the ATES system is not thermally balanced. As shown in Fig. 4.6, the difference between stored cold ( $Q_{load}=1768$  GJ) and heat ( $Q_{unload}=1107$  GJ) was 661 GJ in 2013. An additional 661 GJ of heat therefore had to be supplied to the warm well (32). This can be achieved in several ways, which are explained below.

1. By means of the heat pump

This is the solution described in the design documentation. The roof would then serve as a heat source.

2. By supplying less heat to the roof

An analysis of the roof heating revealed that heat was being delivered even when outdoor temperatures were as high as 8°C, conditions in which there is no risk of ice.

Adapting the outdoor set point and rules could reduce the heat required by 162 GJ.

3. Loading additional heat naturally from the roof

Analysis of the energy data shows that regeneration only took place in July and August, while the ATES system of the HVAC system was in discharge mode, i.e. in cooling mode for the cold water system A. Furthermore, the flow rates of the pumps for regeneration purposes were shown to be very low. By extending the time period and setting the flow rate of the pump to higher speeds, in theory an additional 885 GJ can be generated.

### ***Fault Control ATES***

The cold and warm well temperatures are higher and lower than the designed values. However the lower warm well temperatures in load mode (when heat is delivered by the warm well) do not lead to a significant underperformance of the heat pump: the outgoing water temperatures of the evaporator show no symptoms and the SCOP and the capacity of the heat pump are as expected. In addition, the higher unload cold well temperatures have not led to problems in the cold supply. In light of this, a correction to the control of the ATES system would not lead to significant energy savings.

### **8.2 Primary energy savings**

Here we will discuss the energy savings after correction in terms of primary energy. Fig. 8.1 presents the primary energy consumption before and after corrections. We have assumed that electricity is generated with a mean SCOP of 0.4, which is commonly used in the Netherlands to calculate the primary energy ratio (PER).

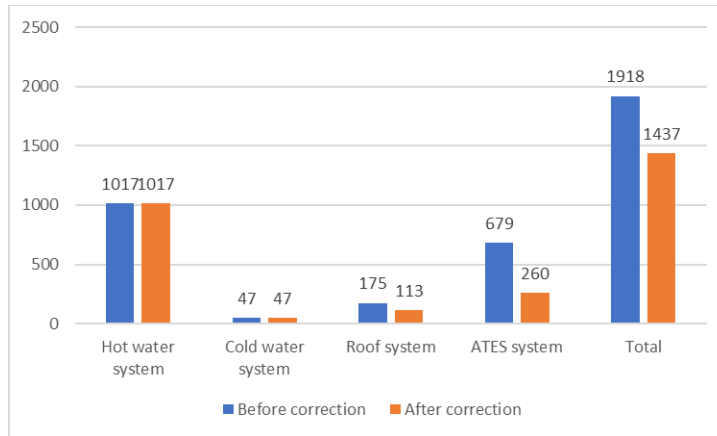


Fig. 8.1 Primary energy consumption for the emitter systems and the ATES system.

The SCOP of components are known from design and actual performance. Before correction, the actual primary energy consumption of the thermal energy plant measured with BMS data from 2013 amounts to 1918 GJ/yr. After the adjustments described in Section 8.1, we see that the primary energy consumption is 1437 GJ / year due to the reduction of energy consumption for the roof and to a large extent for the ATES system. Thus, a primary energy saving of 481 GJ/yr (25.1%) is plausible, even though the thermal energy plant was assessed beforehand by experts and facility managers as performing well.

## 9. Sensitivity analysis of the assumed probabilities in the fault layer

The prior fault probabilities of components and controls are difficult to estimate due to the lack of information about failures. Below, a sensitivity analysis is carried out to estimate the importance of accurate prior probabilities.

Table 9.1 presents the results of this experiment. In the case study, the prior Absent probabilities were set to 98% for components and 95% for the control rules. The prior fault probabilities for all control nodes vary for the sensitivity analysis.

The results of 5 faults for the reference probabilities are presented in the highlighted column 2 in Table 9.1.

Table 9.1 Influence of prior probabilities on the outcomes of the posterior fault Present probabilities

	Prior Absent probabilities		
Components	98	98	98
Control rules	90	95	99.9
	Posterior fault Present probabilities		
<i>Control hot water</i>	100	100	100
<i>Control ATES system</i>	100	100	100
<i>TSA roof system</i>	0	0	2
<i>Control regeneration</i>	100	100	100
<i>Control roof heating</i>	100	100	98

The second and fourth columns show the results for the posterior probabilities, with the prior fault Absent probabilities of the control systems being 90 and 99.9%. The latter is extremely high compared to the component probabilities because experience with HVAC maintenance has shown that control faults occur more often than component errors.

Nevertheless, the 4 control faults are still isolated correctly among a wide range of prior probabilities.

Given the simplicity and limited scope of our analysis, it is remarkable that in our experiments the Bayesian method correctly identifies possible faults even when the absolute values of prior and conditional probabilities are unknown. However, the sign of the differences (positive or negative) between prior probabilities helps in achieving a more accurate diagnosis. In practice, the HVAC maintenance technician is very knowledgeable about the frequency of faults present and this knowledge should be used by the HVAC engineers in designing the DBN. Alternatively, libraries of these values could be set up.

## **10. Conclusions and recommendations**

In this article, the focus is on the fault diagnosis phase based on the 4S3F architecture. In the fault diagnosis phase symptoms identified on the basis of balance, EP and OS indicators (e.g. efficiency, performance factors, capacity indicators) are fed into a DBN model constructed from the P&ID. This DBN model is built from predefined DBN models of aggregated systems (generator, hydronic and emitter systems) and corresponding subsystems (components and control systems).

### **10.1 Results from the case study**

The potential of the fault diagnosis method has been demonstrated in the case study for a thermal energy plant with an ATES system. A full year was covered to show how faults can be isolated automatically.

Although the 4S3F system normally considers three types of faults, for the sake of demonstration only two types of faults were included: component faults caused by faulty capacity, efficiency degradation or component failure, and control faults such as the incorrectly set point of a controller or the inaccurate control of a process mode. For the sake of simplicity, the prior fault Absent probabilities of all components were set to 98% and those of all control rules to 95%. In addition, all conditional fault Present probabilities were set to 95% when a symptom is present.

The proposed 4S3F framework was successful in diagnosing faults in a thermal energy generation plant. It shows that the results are adequate even when prior and conditional probabilities in the DBN nodes are assumed. A sensitivity analysis showed that other

prior values lead to the same fault diagnosis results. Energy savings of up to 25% are possible after fault corrections.

In addition to the results of the energy performance diagnosis of the HVAC system examined, the article proposes a general approach for setting up a library of diagnosis models. These models for systems can be applied to other installations.

## **10.2 Recommendations**

- Although the results are very promising, further research is desirable to extend the framework, improve its accuracy and make it even easier for practitioners to use. The diagnosis aspect of the framework should be applied to other systems, such as air handling systems and heat and cooling facilities in rooms.
- A guideline for the necessary dataset of the BMS needs to be drawn up to estimate energy amounts to and from systems.
- A generic library of diagnosis models is needed from which DBN models can be selected in specific cases. For the sake of this paper, we initiated such a generic library. A relevant research objective would be to detect the strong and weak relationships between symptom and fault nodes.
- Software is needed to implement the state values of the symptom nodes in the DBN model, feed in the set probabilities of the nodes, interface with the DBN model and automate the output of the DBN diagnosis.
- In this case study, GeNie has been used as the DBN software tool. Research is needed to identify the most suitable software tool, capable of handling the libraries of DBN models and redundant symptom information in the right way.

The software must be able to deal with the adapted probabilities of events based on information from data mining and should be suited to implementation in BEMS.

- In this case study, only main heat exchange components (heat pump, boiler, heat exchangers) were considered to be faults. The DBN model can be extended with fault nodes for all components at Level C (e.g. piping, pumps and valves).
- Further research is needed on implementation in DBN. In this paper, Boolean events (Present and Absent) were implemented, meaning that the prior and conditional probabilities give the probability of the event being Present or Absent. When more events for fault and symptom nodes are introduced, it may be possible to estimate the kind of fault, for instance in the case of a negative or positive deviation. It may then also be possible to weigh the degree of the estimated deviation. This can help influence the correction of faults.
- Lastly, research into ways of automating the evaluation aspect of the diagnosis should be conducted. The application of energy balance and EP symptoms in the detection phase ensures the availability of energy levels and performance indicators, which helps to estimate energy savings by corrections.

In future, research should be carried out to see whether the HVAC can be started up automatically by the BMS in a range of modes to speed up the estimation of a fault. For instance, the BMS could estimate bias errors in temperature sensors by starting the pumps and fans at night or at weekends when no heat or cold is needed. Faulty control rules could then also be observed.

## Appendix A

### Control systems for roof heating, and cold water, hot water, condenser and evaporator supply temperatures

#### *Control roof heating system*

The roof is heated when outdoor temperatures are low. Pumps in the roof system extract heated cold water from the hydronic cold water system G. The control for this purpose is presented in Fig. A.1.

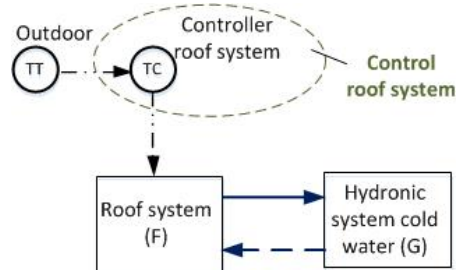


Fig. A.1. Control roof heating system

#### **Control cold water supply temperature (*Control cw*)**

Fig. A.2 is a schematic of the control of the cold water supply temperature of the cold water system G (*Control cw*). As the schematic shows, the controller of the cold water supply activates the ATEs systems (pump CP02-01 is turned on and off). The set point of the cold water supply temperature is based on the outdoor temperature. This cold water supply temperature is measured by TT29-02 and is controlled by the three-way valve TCV29-01 (depicted in Fig. 3.1) in the hydronic system cold water G. When the supply temperature is not reached, the heat pump is set to deliver additional cooling.

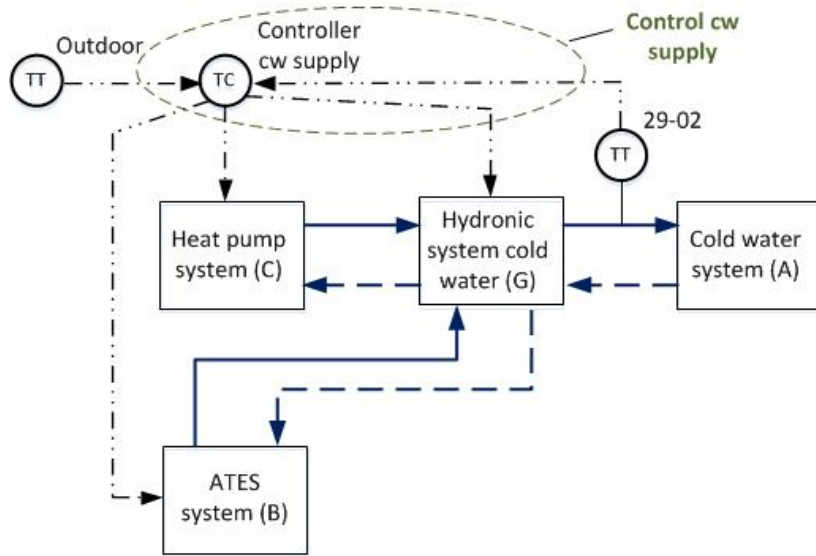


Fig. A.2. Control of the supply temperature of the cold water system

**Control hot water supply temperature (*Control hw*)**

The hot water supply temperature to system E is measured by sensor TT28-02 and controlled by the controller of the outlet condenser temperature at the heat pump. However, when the set point value is not reached, the boiler system is turned on to derive the desired set point value. See Fig. A.3. in which *Control hw* is shown.

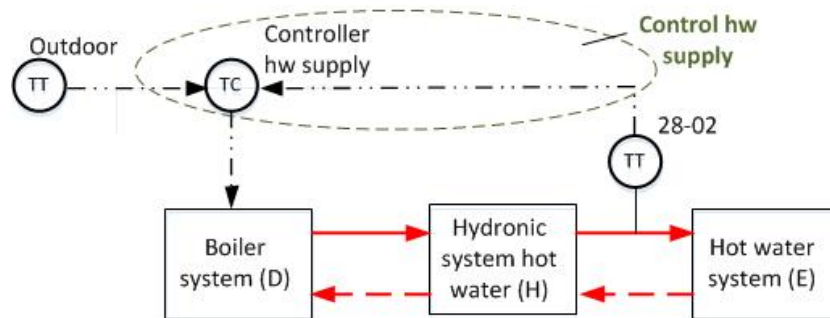


Fig. A.3 Control of the supply temperature of the hot water system

**Control condenser outlet temperature (*Control cond*)**

The control of the condenser outlet temperature of the heat pump (*Control cond*) is presented in Fig. A.4. The outlet condenser temperature is measured by TT04-01 and the heat pump system is controlled using set points and depends on the outdoor temperature.

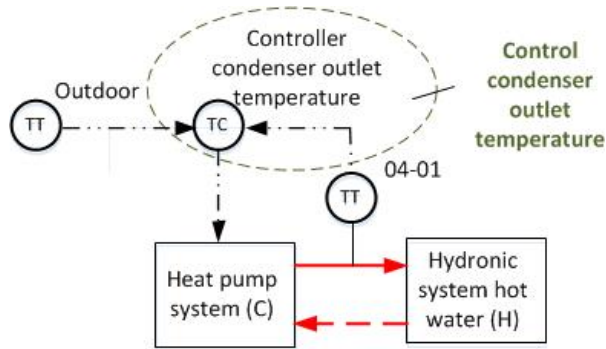


Fig. A.4 Control of the condenser outlet water temperature

**Control evaporator outlet temperature (*Control evap*)**

The evaporator outlet temperature is controlled by TT04-04 and a controller. See Fig. A.5 in which *Control evap* is shown.

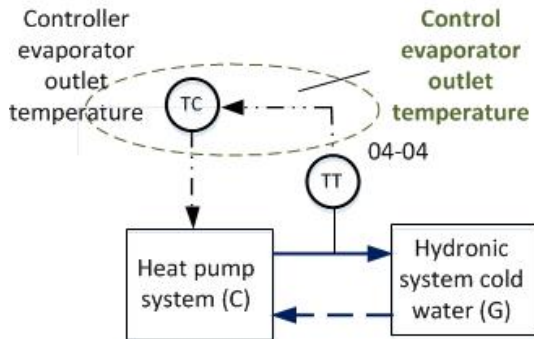


Fig. A.5 Control of the evaporator outlet water temperature

## Appendix B

### DBN models with only aggregated systems A to H without capacity or OS symptoms

In this appendix, DBN models are presented at Level B with and without capacity or operational state symptoms. Fig. B.1 presents the DBN model without capacity symptoms and Fig. B.2 without OS symptoms. Fig. B.3 then shows the DBN model without both capacity and OS symptoms. In this model, only performance indicators are present.

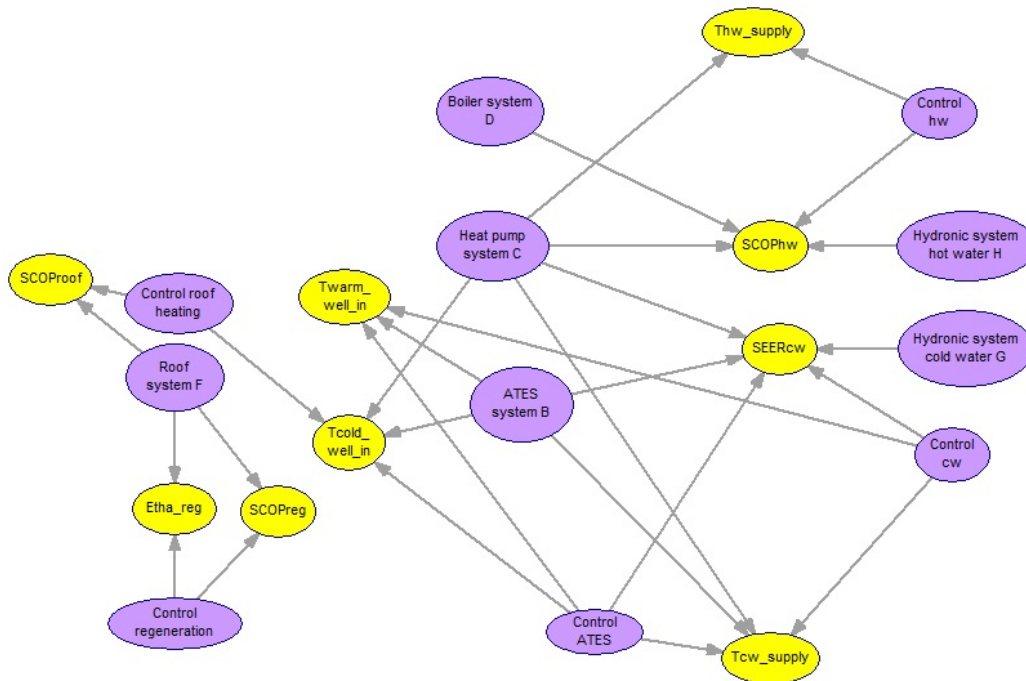


Fig. B.1 DBN model at Level B without capacity symptoms

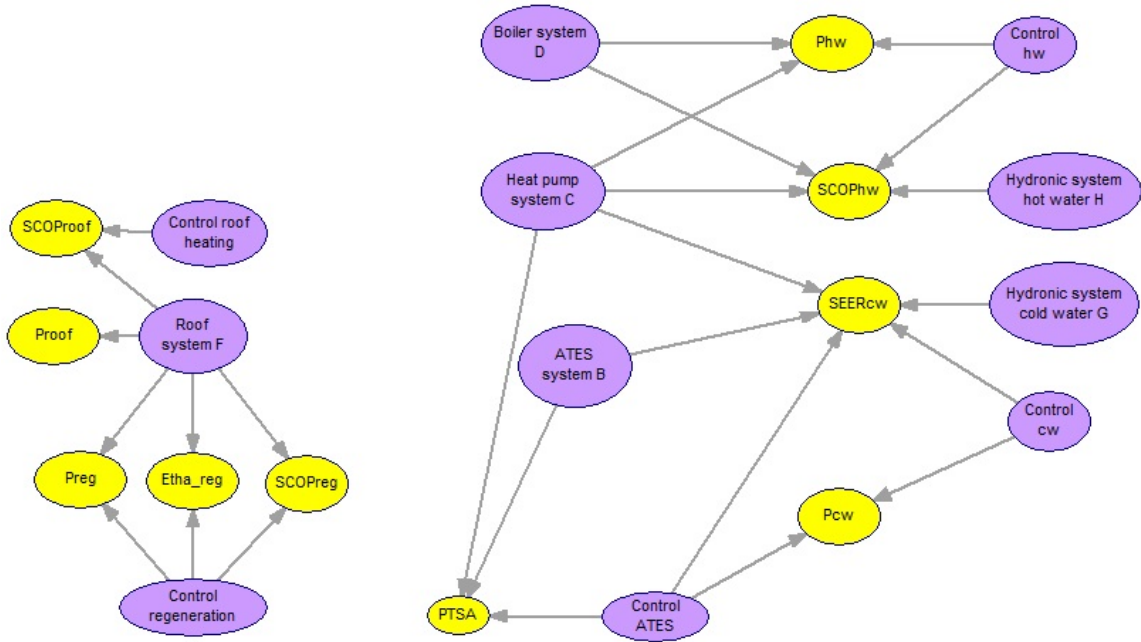


Fig. B.2 DBN model at Level B without Operational State symptoms

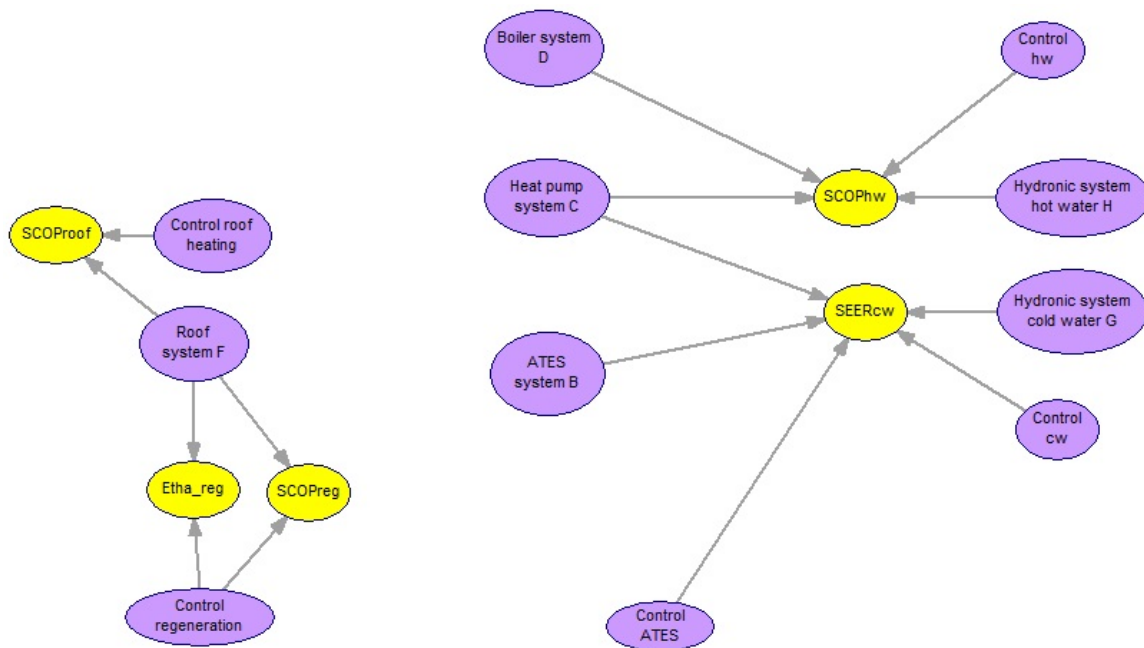


Fig. B.3 DBN model at Level B without capacity and Operational State symptoms

## References

- [1] N. Djuric, V. Novakovic, Review of possibilities and necessities for building lifetime commissioning, *Renewable and Sustainable Energy Reviews* 13 (2009) 486-492.  
<https://doi.org/10.1016/j.rser.2007.11.007>.
- [2] A. Taal, L. Itard, W. Zeiler, A referenced architecture for the integration of automated energy performance fault diagnosis into HVAC systems, *Energy & Buildings* 179 (2018) 144-155. <https://doi.org/10.1016/j.enbuild.2018.08.031>
- [3] W. Kim, S. Katipamula. A Review of Fault Detection and Diagnostics Methods for Building Systems. *Science and Technology for the Built Environment*, 24:1, 3-21,  
<https://doi.org/10.1080/23744731.2017.1318008>.
- [4] S. Wang, F. Xiao. AHU sensor fault diagnosis using principal component analysis method. *Energy and Buildings* 36 (2004) 147–160.  
<https://doi.org/10.1016/j.enbuild.2003.10.002>
- [5] A. Beghi, R. Brignoli, L. Cecchinato, G. Menegazzo, M. Rampozzo, F. Simmini. Data-driven Fault Detection and Diagnosis for HVAC water chillers. *Control Engineering Practice* 53 (2016) 79-91. <https://doi.org/10.1016/j.conengprac.2016.04.018>
- [6] G. Li, Y. Hu, H. Chen, H. Li, M. Hu, Y. Guo, S. Shi, W. Hu. A sensor fault detection and diagnosis strategy for screw chiller system using support vector data description-based D-statistic and DV-contribution plots. *Energy and Buildings* 133 (2016) 230–245.  
<https://doi.org/10.1016/j.enbuild.2016.09.037>
- [7] S. Wang and J. Cui, A Robust Fault Detection and Diagnosis Strategy for Centrifugal Chillers, *HVAC&R Research*, 12:3, 407-428, DOI: [10.1080/10789669.2006.10391187](https://doi.org/10.1080/10789669.2006.10391187)

- [8] J. Liang, R. Du, Model-based Fault Detection and Diagnosis of HVAC systems using Support Vector Machine method. *International Journal of Refrigeration* 30 (2007) 1104.  
<https://doi.org/10.1016/j.ijrefrig.2006.12.012>
- [9] Y. Song, Y. Akashi, J. Yee. A development of easy-to-use tool for fault detection and diagnosis in building air-conditioning systems. *Energy and Buildings* 40 (2008) 71–82.  
<https://doi.org/10.1016/j.enbuild.2007.01.011>
- [10] X. Zhao, Lab test of three fault detection and diagnostic methods' capability of diagnosing multiple simultaneous faults in chillers, *Energy and Buildings* 94 (2015) 43–51. <https://doi.org/10.1016/j.enbuild.2015.02.039>
- [11] N. Ferretti, M. Galler, S. Bushby, D. Choinere. Evaluating the Performance of DABO and HVAC-Cx Commissioning Tools using the Virtual Cybernetic Building Testbed. *Science and Technology for the Built Environment*, 21(8) (2015), 1154-1164.  
<https://doi.org/10.1080/23744731.2015.1077670>
- [12] S. Farouq, S. Byttner, M. Boughalia, N. Nord, H. Gadd, Large-scale monitoring of operationally diverse district heating substations: A reference-group based approach. *Engineering Applications of Artificial Intelligence* 90 (2020) 103492.  
<https://doi.org/10.1016/j.engappai.2020.103492>
- [13] Y. Zhao, F. Xaio, S. Wang, An intelligent chiller fault detection and diagnosis methodology using Bayesian belief network. *Energy and Buildings* 57 (2013) 278–288.  
<https://doi.org/10.1016/j.enbuild.2012.11.007>
- [14] F. Xiao, Y. Zhao, J. Wen, S. Wang, 'Bayesian network based FDD strategy for variable air volume terminals', *Automation in Construction* 41 (2014): 106-118.  
<https://doi.org/10.1016/j.autcon.2013.10.019>

- [15] Y. Zhao, J. Wen, F. Xiao, X. Yang, S. Wang, Diagnostic Bayesian networks for diagnosing air handling units faults – part I: Faults in dampers, fans, filters and sensors. *Applied Thermal Engineering* 111 (2017): 1272-1286.  
<https://doi.org/10.1016/j.applthermaleng.2015.09.121>
- [16] Y. Zhao, J. Wen, S. Wang, ‘Diagnostic Bayesian networks for diagnosing air handling units faults – Part II: Faults in coils and sensors,’ *Applied Thermal Engineering* 90 (2015): 145-157. <https://doi.org/10.1016/j.applthermaleng.2015.09.121>
- [17] EN 15316-1:2017. Energy performance of buildings - Method for calculation of system energy requirements and system efficiencies - Part 1: General and Energy performance expression, Module M3-1, M3-4, M3-9, M8-1, M8-4.
- [18] ISSO-publicatie 44. Het ontwerp van hydraulische schakelingen voor verwarmen. ISSO. 1998. ISBN: 978-90-5044-064-6
- [19] ISSO-publicatie 47. Ontwerp van hydraulische schakelingen voor koelen. ISSO. 2013. ISBN: 978-90-5044-112-4
- [20] A. Taal, L. Itard, Fault detection and diagnosis for indoor air quality in DCV systems: Application of 4S3F method and effects of DBN probabilities. *Building and Environment* 174 (2020) 106632. <https://doi.org/10.1016/j.buildenv.2019.106632>
- [21] GeNie 2.1, BayesFusion. <http://download.bayesfusion.com>, 2016 [accessed 21.04.16].